diversity

MDPI

Article

Using Paleoecological Data to Inform the Conservation Strategy for Floristic Diversity and *Isoetes taiwanensis* in Northern Taiwan

Liang-Chi Wang [1,2]

[1] Department of Earth and Environmental Sciences, National Chung Cheng University, Chiayi 621, Taiwan; lcwang@ccu.edu.tw
[2] Environment and Disaster Monitoring Center, National Chung Cheng University, Chiayi 621, Taiwan

Abstract: Paleoecological data can be used to inform nature conservation practice. Dream Lake (DL) is the best-preserved peat bog in the Tatun Volcanic Group of northern Taiwan. We analyzed continuous pollen and charcoal data from a well-dated sediment core from DL to reconstruct the changes in climate, lacustrine condition, and floristic diversity during the last 4500 cal BP. An absence of volcanic ash from all sediments indicates weak volcanic activity. Significant changes in lithology and pollen composition show that DL changed from a deep lake to a shallow peat bog from 3000 cal BP onwards. The palynological diversity index was negatively correlated with fire frequency. A substantial decline in *Isoetes* (quillwort) spores suggests increased vulnerability during the peat bog period. Natural terrestrialization will lower the mean water depth of DL below the minimum required for *Isoetes taiwanensis* survival within 300 years. Our findings indicate that winter precipitation driven by intense East Asian winter monsoons is the critical force determining the long-term variation in floristic diversity and abundance of *I. taiwanensis*. This long-term ecological history of DL, derived using paleoecological techniques, will be used to inform conservation practice in the Tatun Volcanic Group.

Keywords: vegetation history; wildfires; paleoecology; conservation; peat bog

Citation: Wang, L.-C. Using Paleoecological Data to Inform the Conservation Strategy for Floristic Diversity and *Isoetes taiwanensis* in Northern Taiwan. *Diversity* **2021**, *13*, 395. https://doi.org/10.3390/d13080395

Academic Editor: Tao Su

Received: 23 July 2021
Accepted: 20 August 2021
Published: 22 August 2021

1. Introduction

Peat bogs are extremely sensitive to hydrological changes. They preserve long-term records of the local and regional environment and can help explain trends in the stability, vulnerability, and potential of the ecosystem. As sources of historical information about biodiversity, peat bogs are valuable natural sites of high conservation concern [1].

The Tatun Volcanic Group (TVG) is located in northern Taiwan above the western boundary of the subducting Philippine Sea Plate. It includes more than twenty volcanoes with elevations of 200–1120 m. The TGV is considered active because some geological evidence suggests the presence of an active magma chamber beneath it [2]. Because of the many topographical depressions caused by volcanic activity and high monsoonal precipitation, it is a region of wetland complexes, especially in the rainy season. Several explosion craters are located on Mt. Cising, in the central TVG, some of which have become peat bogs, and the largest and best-preserved of these is Dream Lake (DL).

Dream Lake is protected as an important wetland in Yangmingshan National Park. A rich aquatic biota exists here, including small populations of two endemic species: the quillwort *Isoetes taiwanensis* and the pipewort *Eriocaulon sexangulare*. DL is the only natural habitat of *I. taiwanensis* that is classified as a critically endangered species in the IUCN Red List. It was close to extinction in 2006, and sustainable practices for the conservation of this aquatic fern are urgently needed [3].

According to the monthly observation data of coverage rate of potential competitive plant species and hydrological records in DL, the ideal annual mean water depth for the *I. taiwanensis* population is 50 cm [3]. Since the hydrological condition is the critical factor for

the *I. taiwanensis* population, the information of the development process of DL and the climate condition in the past may contribute to sustained conservation of *I. taiwanensis* in TVG during recent warming.

In spite of the considerable accumulation of palynological records in Taiwan, very few have been recovered from the TVG, because of disturbances from volcanic activity, human impact, and extreme climatic events [4,5]. This lack may impede effective conservation, because the ecological assumptions that are used to inform conservation practices should be subjected to paleoecological scrutiny.

The previous palynological analysis in DL sediments suggested the appearance of *I. taiwanensis since* the lake was formed [6]. However, due to the insufficient ^{14}C dates and relatively low subsample resolution (20–30 cm interval), the paleoenvironmental reconstruction of DL is still lacking [5]. The paleoenvironment of Mt. Cising over the last 1300 cal BP was inferred by pollen, diatom, and geochemical data from a seasonal peat bog near DL [4]. The fluctuation in these multi-proxy data shows late Holocene climate changes and the human invasion during the past 400 years in northern Taiwan.

Pollen and charcoal are the most commonly used proxies for reconstructing vegetation structure and fire disturbances [7]. Here, we integrated pollen and charcoal data to reconstruct the development process of DL, changes in local plant diversity, and wildfire frequency, reflecting the climate patterns in northern Taiwan. Understanding the drivers of changes in plant diversity and the *I. taiwanensis* population during the late Holocene can help to improve the development of nature conservation strategies for Yangmingshan National Park under climate-warming scenarios.

2. Materials and Methods

2.1. Study Area and Sampling

The bedrock of the TVG consists mainly of Pleistocene andesite, volcaniclastic rocks, and Miocene quartz sandstones [8]. The local climate typical of this subtropical zone, with a strong monsoonal influence and distinct wet–dry seasons. Most precipitation falls in August–December. The mean annual temperature in the region is 18.8 °C, mean annual rainfall is 4143.7 mm, and mean annual relative humidity is 86.1% (data from Zhuzihu Weather Station, 1991–2020).

The vegetation of northern Taiwan is strongly affected by the winter monsoon, which brings abundant rainfall and markedly lower temperatures. The timberline in central Taiwan is at ~3600 m, but it descends to 1000 m in northern Taiwan [9]. According to the local vegetation map (Figure 1), the natural vegetation is low montane grassland (Miscanthus grassland), low montane shrub (dwarf bamboo), and lowland forest (broad-leaved forest). *Miscanthus sinensis* var. *glaber* and *Arundinaria usawai* are the dominant species in low montane grassland and low montane shrub, respectively, which are distributed above the timberline at an elevation of ~800 m. *Machilus thunbergii*, *Machilus japonica*, *Trochodendron aralioides*, and *Liquidambar formosana* are the main components of lowland forests at altitudes of 200–900 m. *Cryptomeria japonica* and *Acacia confusa* are the main species of the secondary forest.

The DL basin has an area of 0.5 ha, with a watershed of 4.34 ha. The annual mean water depth is 39.4 cm, and the submerged area varies from 0 to 0.32 ha [3]. Local precipitation and groundwater discharge are the primary water inputs. The distinct seasonal difference in rainfall strongly affects the water table, water area, and vegetation coverage in the DL wetland [10]. During the wet season of 2013, the coverage area of Poaceae (*Miscanthus sinensis* var. *glaber*) and Cyperaceae (*Eleocharis congesta*, *E. dulcis*, *Schoenoplectiella mucronata*) declined, while that of *Isoetes taiwanensis* increased gradually (Figure 2).

Deforestation in the TVG occurred during 1875–1942. The natural lowland forests were replaced with tea cultivation, rice paddies, and orchards, but the level of human disturbance near DL was relatively low. In 1972, the Taipei City government developed DL as a scenic area and created a plantation of an exotic conifer, Cryptomeria japonica, beside DL (Figure 3). In 1985, the Yangmingshan National Park was promulgated, and the

Dream Lake Ecological Reserve was established to protect the endemic *I. taiwanensis*. In 1992, the *I. taiwanensis* population decreased dramatically, because DL had dried up. In 1993, Yangmingshan National Park authorities dredged DL to increase the aquatic habitat of this endemic species.

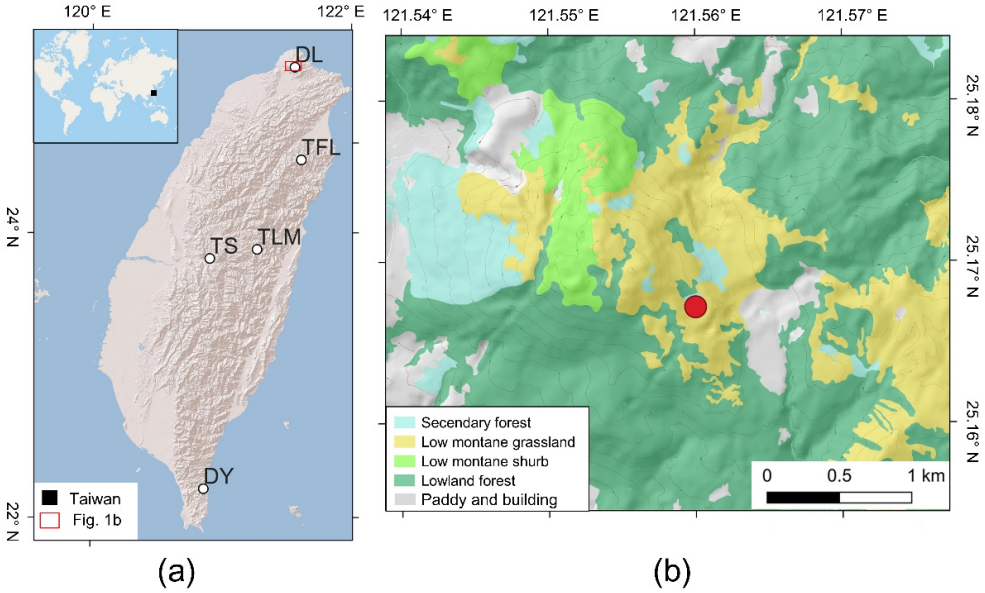

Figure 1. (**a**) Locations discussed in the text (white circles): Dream Lake (DL), Tsuifong Lake (TFL), Tunlumei Pond (TLM), Toushe Basin (TS), and Dongyuan Lake (DY). (**b**) The local topography and vegetation around DL (red circle).

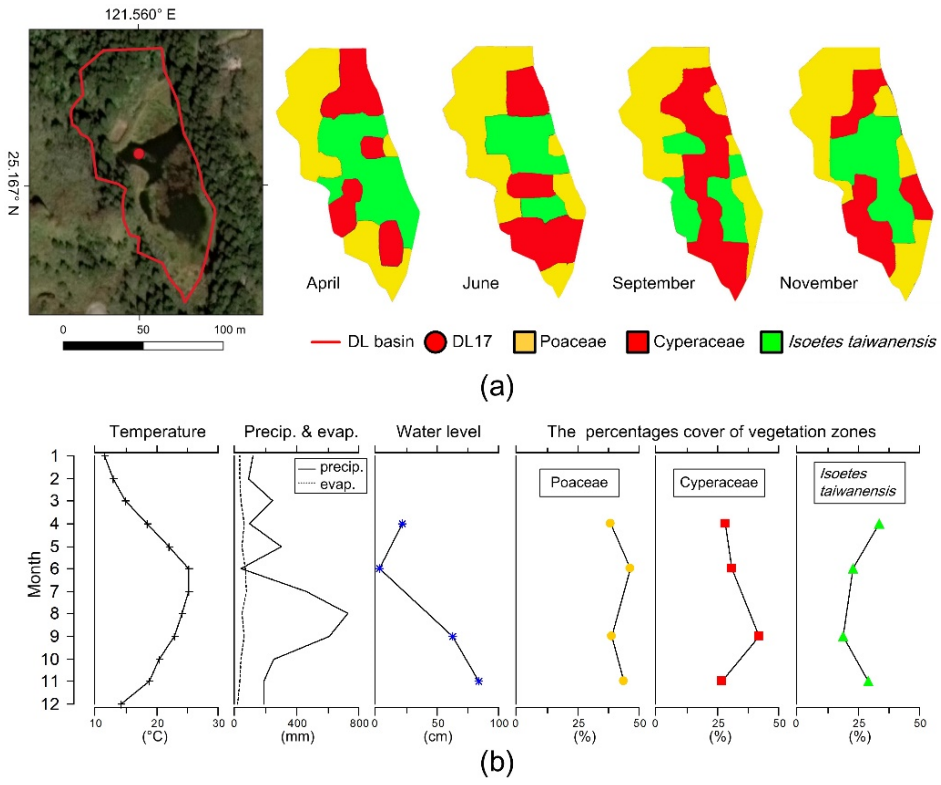

Figure 2. (**a**) Satellite photograph of coring site (red circle) and the spatiotemporal distribution of wetland vegetation in the Dream Lake (DL) basin in 2013. (**b**) Mean monthly temperature, precipitation, evaporation, water level, and percentage cover of three vegetation types in DL in 2013 [10].

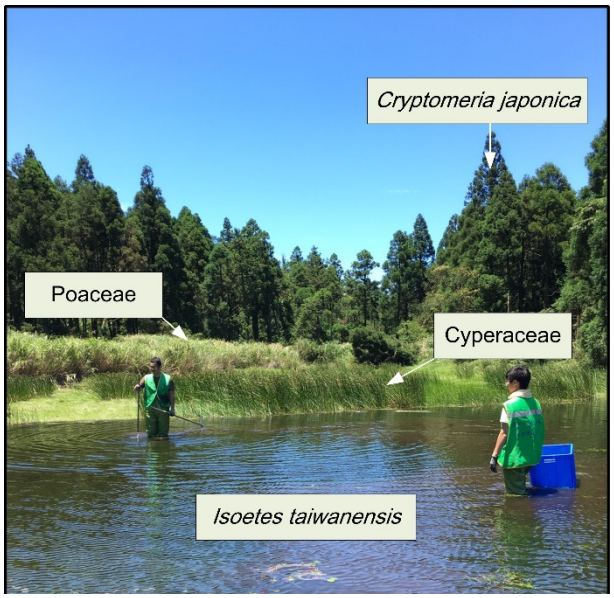

Figure 3. Dream Lake wetland in July 2017. The exotic conifer species *Cryptomeria japonica* is present along the shores of the wetland. The vegetation zones characterized by Poaceae, Cyperaceae, and *Isoetes taiwanensis* can be seen.

A 180 cm sediment core (DL17, 25°10′01.9″ N, 121°33′36.0″ E) was drilled from the northern part of DL at a water depth of 50 cm in July 2017, using a 50 cm-long, 5 cm-diameter Russian sampler (Figure 2). The sediments were subsampled at 2 cm intervals to obtain 90 samples for use in pollen and charcoal analysis. Seven samples were chosen for accelerator mass spectrometry (AMS) radiocarbon dating and submitted to the NTUAMS Lab, Taiwan. The age–depth model was constructed using Bayesian statistics, as implemented in package "rbacon" in R, using the IntCal20 calibration curve [11–13].

2.2. Multiproxy Analysis and Paleo-Floristic Diversity Assessment

We used fossil pollen and charcoal analysis, pollen diversity estimates, ecological ordination techniques, and fire frequency analysis to reconstruct the vegetation history and fire frequency at DL. This would reflect regional climatic trends and their impacts on the local floristic diversity.

For pollen analysis, a 0.5 cm^3 core subsample was treated with 10% KOH, 10% HCl, 40% HF, and an acetolysis mixture. Before chemical treatment, one *Lycopodium* spore tablet of known spore concentration was added to calculate the pollen concentration (grains cm^{-3}). Acetolyzed pollen material was concentrated by sieving with a 5 µm nylon mesh filter in an ultrasonic bath. The pollen concentrate was mounted in glycerol jelly. The pollen taxonomy used for classification mainly followed local usage for pollen and spore floras [14,15]. Pollen percentages were based on the total sums of pollen. Fern spores and microalgae were based on their amounts relative to total pollen counts. For most samples, 300 pollen grains were identified and counted using an optical microscope with 400× magnification. Samples with counts < 100 were considered to exhibit poor pollen preservation and excluded from numerical analysis. Pollen diagrams were produced using Tilia version 2.1. Pollen data were subjected to cluster analysis using the CONISS program of Tilia Graph to identify the local pollen zones [16].

Modern pollen richness is known to be positively correlated with contemporary plant species richness [17], and past floristic diversity can thus be inferred from fossil pollen records [18]. To estimate the past diversity of the vegetation surrounding DL, we used three different pollen-based indices to measure palynological diversity and evenness. Pollen-type diversity (PDI) was calculated based on a rarefaction analysis of a small sample of pollen taxa; this index is strongly correlated with local floristic diversity within 1 km of the deposit [19]. Hill's number (Hill N1) is the effective number of taxa used in the

Shannon–Wiener index, and integrates both the richness and the evenness aspects of the data, thus reflecting diversity [20]. The probability of interspecific encounter (PIE) is the probability that two individual pollen grains selected randomly from a sample belong to different taxa, and it is regarded as an index of palynological evenness [21].

For our ordination analyses, we selected pollen taxa from at least three samples, restricting the taxa to those with a proportional presence of >1% to avoid the effect of rare taxa. The 15 selected pollen taxa were square-root-transformed to reduce the effects of abundant taxa and to stabilize the variance [22]. Detrended correspondence analysis (DCA) was used to determine whether linear or unimodal-based techniques should be used. The length of the gradients was 0.83 standard deviations (SD), which, since it was <2, indicated that principal component analysis (PCA) would be suitable to explore the primary trend in DL vegetation. All numerical analyses of pollen data were carried out in R using the "Vegan" and "mobr" packages [11,23].

For the macroscopic charcoal analysis, subsamples of 2 cm^3 were treated with 12% NaClO for 48 h to digest the organic matter in the sediments, then sieved with a 125 µm mesh [24]. The charcoal particles in each sample were counted and photographed under the stereo microscope to measure the charcoal concentration (pieces cm^{-3}). The total area of all charcoal particles per sample (mm^2 cm^{-3}) was measured using ImageJ 1.52a [25].

We reconstructed the local fire history by analyzing the charcoal data using the CharAnalysis1.1 code for Matlab R2021a [26]. Briefly, we interpolated the raw charcoal count data to a median temporal resolution of 37 years and log-transformed (log10) the interpolated data to assess the charcoal accumulation rate (CHAR, pieces cm^{-2} yr^{-1}) in constant time steps (C_{inter}). We estimated the low-frequency variation in CHAR (C_{back}) using a locally weighted regression with an 800-year window. We calculated the high-frequency CHAR (C_{peak}) as the residual of C_{inter} minus C_{back}. C_{peak} consists of C_{noise} (noise from sediment mixing, sampling, and analyzing) and C_{fire} (actual fire events within 1 km). We used a Gaussian mixture model to identify the C_{noise} distribution and evaluated the threshold as 95% to separate samples into "fire" and "non-fire" events. We smoothed fire frequencies using an 800-year window (fires 800 y^{-1}) to infer the past fire regime condition.

3. Results

3.1. Core Description and Age–Depth Model Construction

The sediment core DL17 consists mainly of organic-rich dark black peat in the upper 88 cm. The lower portion, between 88 and 180 cm, is a mineral substrate consisting of dark-gray silt, gray silt, and light-gray silt (Figure 4).

An age–depth model for the DL sediment was derived from seven radiocarbon dates (Table 1), using Bayesian analysis to produce age estimations with best-fitting uncertainty estimates. In the uppermost 6 cm of sediments, we noted the occurrence of pollen from *Cryptomeria* (Figure 5), an exotic species introduced to the study area in 1931 [27]. The upper sediments were artificially removed to deepen the DL in 1993, and the sediments in the upper 6 cm of DL17 should be considered to have been deposited after this event. Thus, we assumed a human-caused hiatus at 6 cm in the age–depth model of DL17 (Figure 4). The sedimentation rate varied between 0.02 and 0.07 cm yr^{-1}, with an average of 0.05 cm yr^{-1}. Based on the age–depth model, we calculated a peat accumulation rate of 0.03 cm yr^{-1} between the 88 and 6 cm levels, varying from 0.02 to 0.05 cm yr^{-1}. We excluded samples from the upper 6 cm from numerical analysis because of the data discontinuity and the strong effects of contemporary human disturbance.

3.2. Pollen, Charcoal, Biodiversity Estimation, and Ordination Results

The pollen diagram of DL is presented in Figure 5 and shows the most important pollen and spore taxa within their respective vegetation groups. Samples in which pollen was poorly preserved (from below 172, 166, and 100–90 cm) were excluded from numerical analysis; these depths are blanked out in the pollen diagram. Four pollen assemblage zones,

DL1–DL4, were identified based on the CONISS cluster analysis. The pollen, charcoal, and biodiversity estimates for each of these zones are described below.

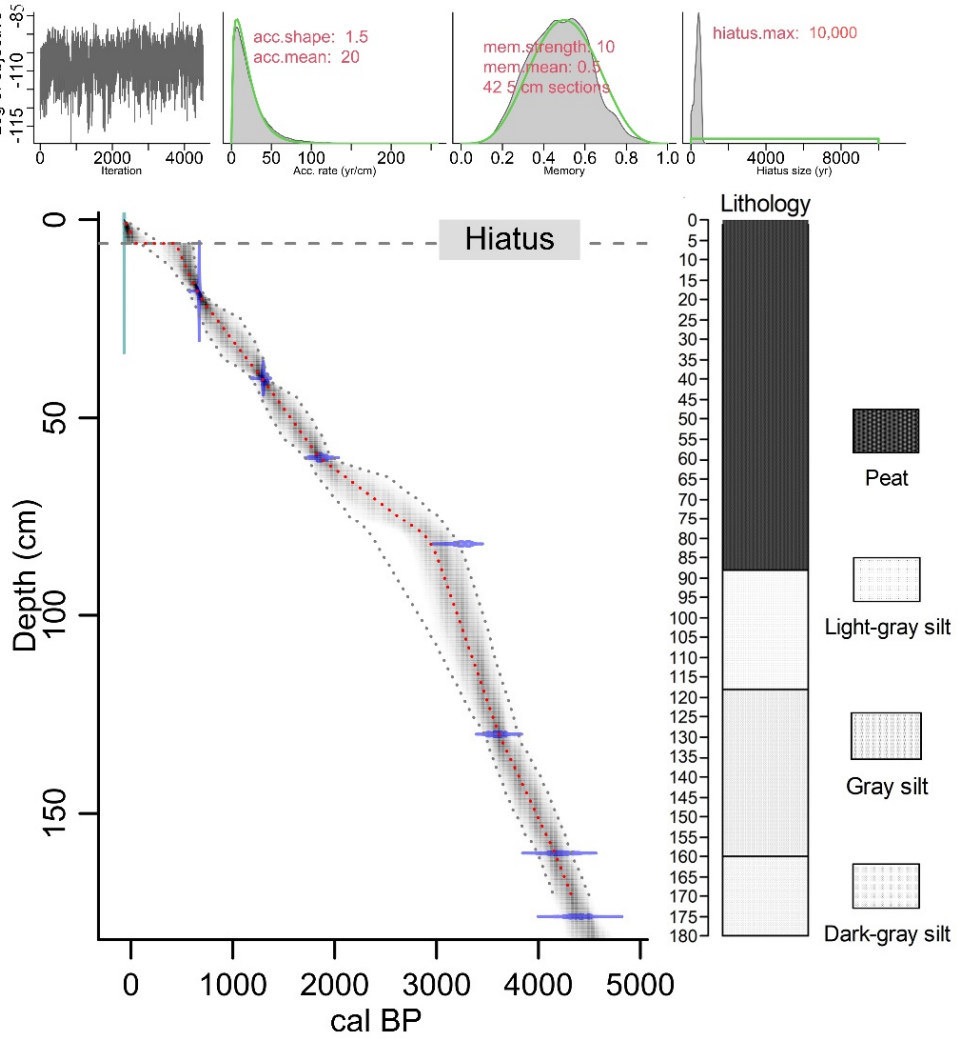

Figure 4. Age–depth model and lithology for Dream Lake generated using Bayesian analysis in package "rbacon" for R [12]. The gray shading indicates the 95% probability intervals for the age models. Seven radiocarbon dates (blue) were used for calibration. The hiatus was set at a depth of 6 cm.

Table 1. Radiocarbon dates estimated for Dream Lake sediments. Calibrated radiocarbon ages with 2σ error were computed using Calib 8.20 (http://calib.org/calib/calib.html, accessed on 1 July 2021), which uses the IntCal20 calibration curve [13].

Lab Code	Sample ID	Depth (cm)	Type of Sample	pMC (%)	^{14}C Age (BP)	Calibrated ^{14}C Age (cal BP)
NTUAMS-4088	DL 18	18	peat	91.41 ± 0.90	722 ± 7	669 ± 6
NTUAMS-4472-1	DL 40	40	peat	84.13 ± 1.13	1389 ± 19	1299 ± 14
NTUAMS-4473-2	DL 60	60	peat	78.56 ± 1.09	1938 ± 27	1857 ± 78
NTUAMS-4089	DL 82	82	peat	68.53 ± 0.88	3035 ± 39	3252 ± 107
NTUAMS-4090	DL 130	130	sediment	65.82 ± 0.70	3359 ± 36	3565 ± 82
NTUAMS-4474-1	DL 160	160	sediment	62.17 ± 0.87	3818 ± 53	4247 ± 162
NTUAMS-4091	DL 176	176	sediment	61.17 ± 0.78	3948 ± 50	4382 ± 141

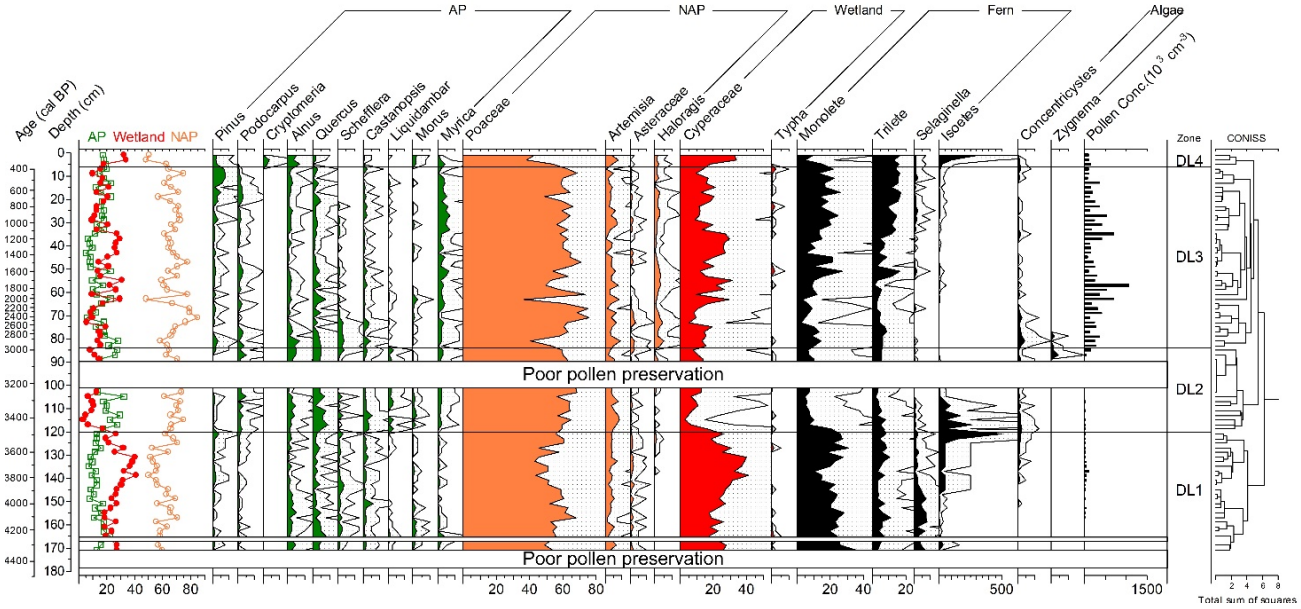

Figure 5. Profile diagram of pollen percentages for selected pollen taxa with respect to the four pollen zones in the Dream Lake sediment core. Only taxa present at >1% in at least three samples are plotted. Percentages are based on the sum of all pollen. The shaded area is a five-fold exaggeration of the original values. Three intervals of poor pollen preservation are represented with blank white bars.

DL1 (180–120 cm; 4500–3500 cal BP) is characterized by nonarboreal pollen (NAP) dominance and low pollen concentration. Abundance of arboreal pollen (AP) is low and ranges from 7–17%. *Alnus* (0–5%) and *Quercus* (1–8%) are relatively important. NAP taxa in the Poaceae (48–63%) and *Artemisia* (2–8%) are present at high percentages throughout the period. Wetland pollen taxa in the Cyperaceae (18–39%) increase gradually and reach a maximum at a depth of 133 cm. Fern spores (1–49%) are dominant. The aquatic *Isoetes* is the most dominant fern taxon. The algal taxon *Concentricystes* occurs continuously in the upper part of the zone. CHAR is high in the middle of the zone. PD1, Hill N1, and PIE show opposite trends to the CHAR records (Figure 6).

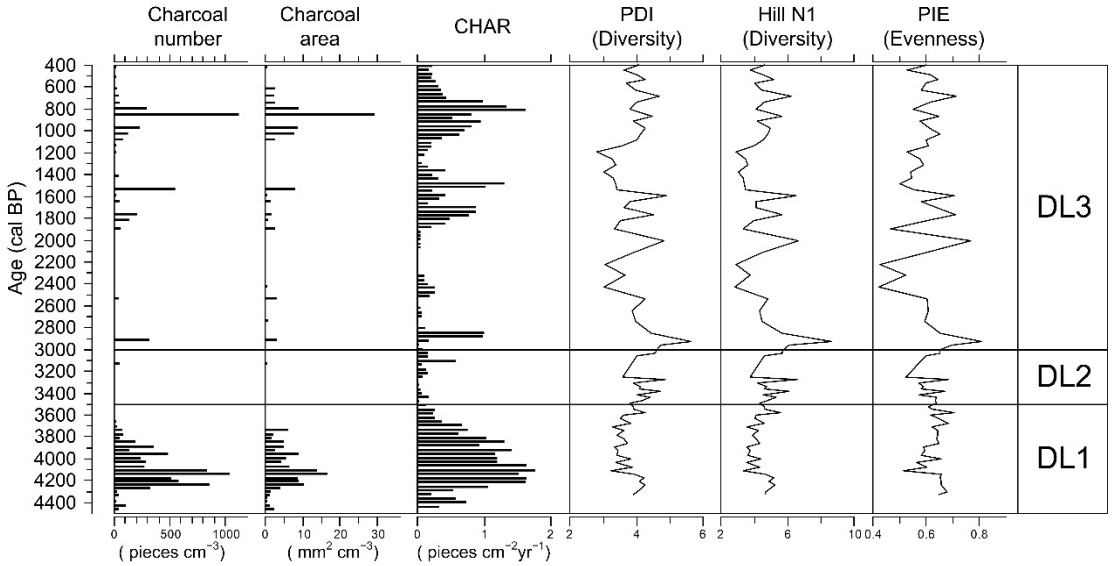

Figure 6. Profile of charcoal concentration (number and area of pieces), charcoal accumulation rate (CHAR), pollen-type diversity (PDI), Hill's number (Hill N1), and probability of interspecific encounter (PIE) with respect to the three pollen zones in the Dream Lake sediment core. DL4 was considered to represent modern deposition and was excluded from the diagram.

Zone DL2 (120–84 cm; 3500–3000 cal BP) covers a period with a pattern of rapid transition. AP (15–30%) is somewhat more abundant than in the previous period, with an average of 22%. *Alnus* (1–6%) and *Quercus* (2–9%) are the dominant tree taxa. Components of lowland forest, including *Podocarpus*, *Castanopsis*, *Liquidambar*, and *Myrica*, increase. NAP (63–74%) remains abundant. Wetland taxa (3–17%) decrease substantially, to 12% on average. Terrestrial fern taxa decrease. However, the aquatic fern Isoetes is abundant, but disappears above the pollen-poor preservation layer. *Concentricystes* still occurs, while *Zygnema* peaks in the top of the zone. Pollen concentration is still low. CHAR is very low, while the three palynology diversity indices increase gradually.

In zone DL3 (84–6 cm; 3000–400 cal BP), AP decreases, and *Myrica* (1–7%) is relatively important. NAP (48–80%) is still dominant, and *Haloragis* (1–5%) becomes more important in this time interval. Among wetland taxa, Cyperaceae (9–22%) increase in the middle of the zone. Fern spores increase gradually toward the recent period. *Concentricystes* occurs intermittently. Pollen concentration is very high, CHAR is much higher than before, the three palynology diversity indices decline overall (with strong fluctuations), and fire frequency is high.

In zone DL4 (upper 6 cm; the recent period), AP (17–20%) varies little. *Alnus* (4–7%) is the most dominant tree pollen. The exotic conifer taxon *Cryptomeria* is present. Among the NAP, Poaceae decrease rapidly, toward 45% on average. Among wetland taxa, Cyperaceae (18–34%) continue to increase, and *Typha* is absent. Fern spores increase, especially *Isoetes*. Pollen concentration is lower than in the previous period.

The first two PCA axes of pollen data are statistically significant, explaining 29.19% and 16.95% of the total variance in the DL pollen data set (Figure 7). PCA axis 1 (PC1) is strongly positively correlated with the Cyperaceae wetland taxa. PC1 may thus be positively related to the area of wetland in the DL basin.

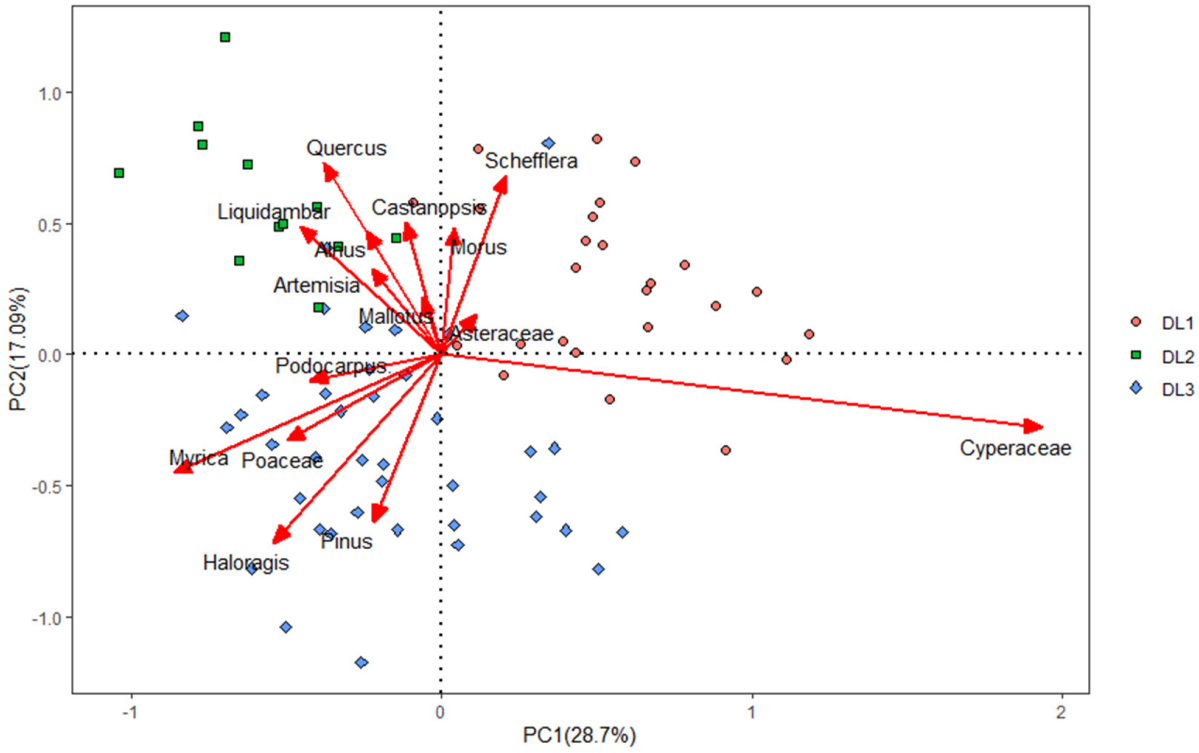

Figure 7. Principal component analysis biplot of the pollen composition of sediments from Dream Lake. The samples in DL4 were considered to represent modern deposition and were removed from the ordination analysis.

4. Discussion

4.1. Paleoenvironment Interpretation and Paleoclimate Reconstruction

Pollen and macroscopic charcoal occur at different spatial scales because of differences in dispersal and deposit processes. Charcoal is relatively macroscopic, although some factors such as fire intensity, upper-level wind speed, and landscape topography, may contribute to its long-distance transport [28]. Pollen can be dispersed up to 20–50 km by wind and may represent the local to regional vegetation [29]. The relevant source area for pollen deposits under fixed atmospheric conditions is mainly correlated to the basin size [30]. The majority of pollen in the sediment of a small lake such as DL comes from the vegetation that is <1 km from the lakeshore, reflecting the local to extra-local vegetation [21,31].

The pollen record of DL shows signals of regional climatic trends and local hydrological changes over the last 4500 cal BP (Figure 8). DL is located above the timberline, where Poaceae dominate. The high percentages of Poaceae throughout the core suggest the presence of a stable grassland landscape near the DL basin. The AP pollen in DL sediments mainly derives from the lowland forest. Hence, the increase in AP may indicate an expansion of the forest zone, reflecting the warm climate in northern Taiwan [4]. According to an analysis of four sets of palynological records from Taiwan, the climate trend during the late Holocene in Taiwan can be summarized as a relatively prominent cold period during 3870–1920 cal BP, the Roman Warm Period during 1920–1590 cal BP, the Migration Period Cooling during 1590–1190 cal BP, the Medieval Warm Period during 1190–650 cal BP, and the Little Ice Age during 650–100 cal BP [32]. We overlaid these warm–cold periods on the AP spectrum in the DL sediments to compare this record with the regional climatic trends in Taiwan (Figure 8).

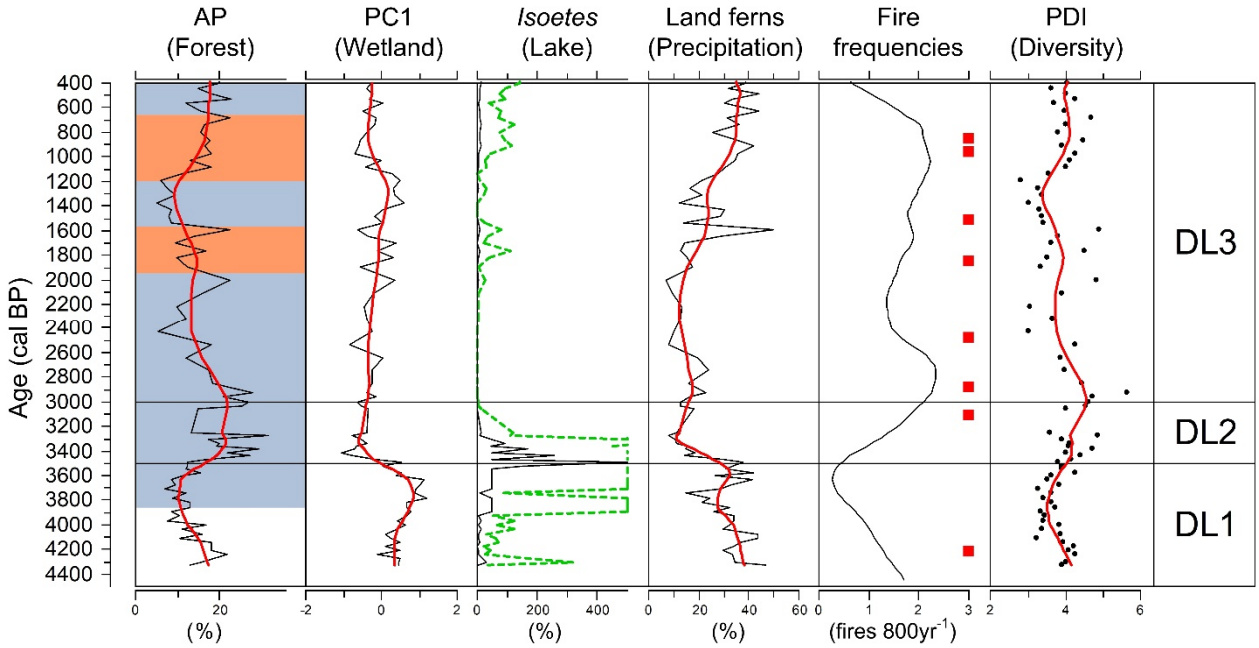

Figure 8. Summary of the paleotemperature (arboreal pollen, AP), wetland area (PC1), water area (*Isoetes*), precipitation (land ferns), fire frequency, and floristic diversity (PDI) of Dream Lake, as inferred from sedimentary proxies, over the last 4500 cal BP. Fire peaks are indicated with red squares. The red lines are smoothed curves generated using the locally weighted scatterplot smoothing method in C2 ver. 1.5 for Windows. The green dashed line is a 10-fold exaggeration of the original values. The background of the AP column indicates the late Holocene climatic conditions in Taiwan (red = warm period; blue = cold period), based on a summary of four palynological records [32].

We used the relative abundance of *Isoetes* as an index of the change in water depth in DL. *I. taiwanensis* is a submerged aquatic plant, and its abundance is positively associated

with water depth [3]. Seasonal fluctuation in the water level may reduce the competition among *I. taiwanensis* and other emergent plants, particularly Cyperaceae. Thus, the interplay between *Isoetes* presence and PC1 can reveal the coverage area of two wetland vegetation types, indicating aquatic conditions.

Land ferns prefer humid habitats. Their spores are heavy, and water transportation is more important for their distribution than wind transportation [33]. The ratio of fern spores and pollen in lacustrine sediments has been widely used to infer humidity conditions and precipitation in Taiwan [34,35]. Therefore, we used the percentages of land fern spores in the DL sediments to infer the changes in precipitation in northern Taiwan. We summarized the precipitation proxies from northern Taiwan (DL), northeastern Taiwan (Tsuifong Lake), central Taiwan (Tunlumei Pond and Toushe Basin), and southern Taiwan (Dongyuan Lake) to investigate the spatiotemporal variability of rainfall during the late Holocene [34,36–38]. The intensity of the East Asian summer monsoon (EASM) is considered the primary force driving precipitation in East Asia during the Holocene [39]. The historical flooding periods along the upper Amur River Delta reflect the six periods of the late Holocene when the EASM was strengthened [40]. These EASM-strengthening periods are marked in Figure 9 to aid interpretation of the influence of the EASM on precipitation patterns in Taiwan.

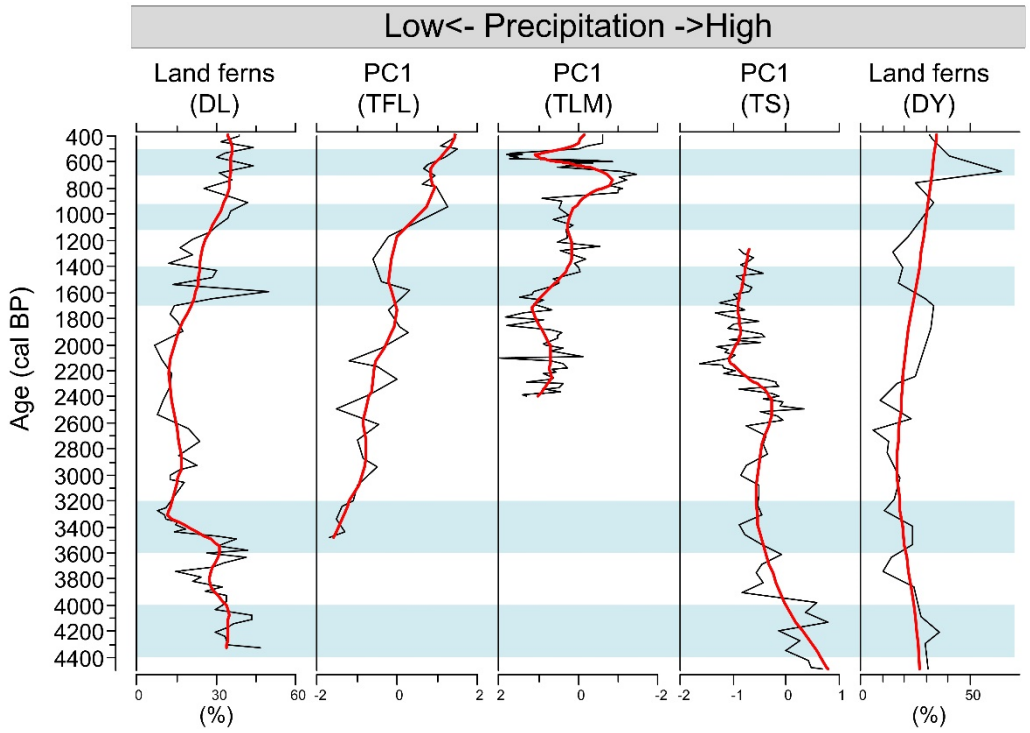

Figure 9. Summary diagram for proxy-inferred paleo-precipitation in northern (DL, this study), northeastern (TFL, [36]), central (TLM, [37], TS, [38]), and southern Taiwan (DY, [34]) over the last 4500 cal BP. The blue bars represent periods of intense East Asian summer monsoon, based on historical records of flooding periods along the upper Amur River Delta [40].

Lakes in the volcanic environment are dynamic and have short-lived features because of volcanic eruptions and related processes [41]. Approximately 6000 years ago, possibly because of a strong earthquake, a large fissure dissected the summit area of Mt. Cising. This earthquake caused small-scale phreatic explosions at several locations along the fissure and induced the gravitational collapse of Mt. Cising [8]. The radiocarbon date of the organic carbon at the upper boundary of the andesite bedrock in the central sediment profile of DL is 5600 cal BP [6]. This confirms that DL is one of those explosive craters that were generated after this eruption. In our records, the poor pollen preservation in the silt sediments exhibiting substantial accumulation during 4500–4400 cal BP may correlate to the rapid deposition period after this eruption. After 4400 cal BP, PC1 and *Isoetes* spores

remain high, reflecting stable lake conditions and a high-water level. The low abundance of AP pollen in DL suggests that the lowland forests were far from the DL basin during this period, indicating a cold climate. The high percentage of land fern spores and the low fire frequency suggest a humid environment. Regional precipitation trends in Taiwan, as inferred from proxy data, generally indicate intense EASM precipitation during 4400–4000 cal BP (Figure 9).

A prolonged dry interval during 4000–2000 cal BP has been reported from the East Asia coast, and this is correlated to a decline in insolation and the failure of EASM rainfall [42]. The intense EASM precipitation during 3600–3200 cal BP observed in the upper Amur River Delta [40] is not clear in the precipitation proxy data for Taiwan, although the rapid decline of land fern spores in DL suggests a decrease in precipitation in northern Taiwan after 3500 cal BP. In contrast to the long-term drying trend suggested by the land fern spores, the strong fluctuations in the substantial *Isoetes* presence and low abundance of taxa correlated with PC1 during 3500–3300 cal BP indicate that the DL basin was mainly filled with water to a substantial depth. The poor pollen preservation layer suggests a rapid input of mineral material from the catchment during 3300–3100 cal BP, which diluted the pollen concentration and reflects flooding [43]. After this period, the absence of *Isoetes* and the occurrence of the microalgae *Concentricystes* and *Zygnema* may imply shallow lake conditions [44].

The water level of DL today is strongly associated with typhoon-triggered precipitation in the summer season (Figure 2). According to lacustrine records from the last 1000 years, typhoons tend to pass through northern Taiwan during La Niña-like periods [45]. This suggests that variations in local precipitation may be modulated via a complex interplay between regional EASM intensity and typhoon track variation in coastal East Asia [46]. The finely laminated sediment records in Bainbridge Crater Lake in the Galápagos Islands indicate frequent La Niña events between 3500 and 3000 cal BP [47]. Thus, the occurrence of high-water levels at DL may be correlated to frequent typhoon events in northern Taiwan during this period, reflecting abrupt local hydrological oscillations rather than long-term regional climate patterns.

The continuous deposition of peat at a low sedimentation rate indicates that, like today, DL was a peat bog in the period 3000–400 cal BP. The decreasing trend in AP and the paucity of land fern spores indicate a cool, dry climate during 3000–2000 cal BP. The low value of PC1 and absence of *Isoetes* spores for that period reveal that at that time, DL was a very shallow bog with a small wetland area.

During the last 2000 cal BP, the pattern of AP abundance follows the warm Roman Warm Period, the cool Migration Period Cooling, the warm Medieval Warm Period, and the cool Little Ice Age. Precipitation proxies in Taiwan all reveal increased precipitation during the last 2000 cal BP (Figure 9). However, the recently intensified EASM is abnormal in the context of the downward trend in Northern Hemisphere insolation [48]. The land fern spores from DL are better correlated with the last three EASM-intense periods than precipitation proxies from other sites, indicating that EASM-associated rainfall events have been the predominant source of water in northern Taiwan during the last 2000 cal BP.

The peaks in *Isoetes* spore abundance are significantly associated with decreased Poaceae and increased Cyperaceae abundance in the uppermost 6 cm of sediments (Figure 5), which we assume is a consequence of the artificial management and recent restoration activities following the dredging in 1993. Yangmingshan National Park management filled in the fissures in the DL shoreline to improve the water level and removed the dominant land herb species (*Miscanthus sinensis* var. *glaber*) from the western section of DL to mitigate terrestrialization.

4.2. Drivers of Local Vegetation Dynamics

In the TVG region, volcanic eruption, human disturbances, and the climate are all potential drivers of wildfires that can impact local floristic diversity. The characterization of the TVG as active and as having a magma chamber beneath it, based on seismic evidence

from dense seismic arrays in northern Taiwan, is still controversial [2,49]. A major eruption in the TVG that produces lava and volcanic ash would strongly affect the landscape and vegetation composition [50]. However, the absence of tephra deposits throughout the DL sediment core reveals that no large eruption has occurred during the last 4500 cal BP.

Anthropogenic disturbances such as slash-and-burn agriculture and forest management have been the principal drivers of fires in lowland Taiwan, especially during the late Holocene [7,51]. Intensive human activity can be inferred from the occurrence of cultivated plant pollen and charcoal in sediments. The lack of such pollen in the DL sediments suggests a low level of human activity, and the charcoal records are thus likely to reflect nature wildfires.

Precipitation levels control fuel moisture, while strong winds can encourage fires [52]. Climatic conditions, especially fluctuations in precipitation, are associated with high variability in fire frequency. However, land fern spores at DL are poorly correlated with fire frequency (Figure 8), revealing the relatively weak impact of EASM-induced precipitation. More than 84% of fires in subtropical China happen during winter, from January to April, based on continuous observation data from multiple satellites collected during 2005–2018 [53]. We therefore propose that the intensity of winter monsoonal precipitation may be the driver of local fires in subtropical Taiwan.

The palynological diversity index (PDI) and AP curves are very similar (Figure 8). The DPI is more sensitive to the variation of lowland forests. It may be due to the higher floristic diversity in lowland forests than in low montane grassland. The small fires near DL may increase charcoal concentration but had little impact on DPI. Thus, the DPI and fire frequency with an opposite trend can assume the large fires and strong disturbances in northern Taiwan.

PDI is low when fire frequency is high, and it tends to decrease after individual fire events (Figure 8). This confirms that fire events have a strong effect on local floristic diversity in northern Taiwan. Diversity is a compound concept that includes species richness and species evenness. The similar pattern in two diversity indices (PDI and Hill N1) and one evenness index (PIE) suggests that the floristic diversity in DL is strongly linked to species evenness rather than species richness. Fire frequency in northern Taiwan is strongly correlated to the intensity of winter precipitation. Understanding future trends in winter monsoon intensity under global warming scenarios could be key to the conservation of floristic diversity in a dynamic environment such as the TVG.

4.3. Implications for Isoetes taiwanensis Conservation

Our palynological records for DL enabled us to reconstruct the development process of the wetland and its impact on the *I. taiwanensis* population. The numerous *Isoetes* spores in the early stages, when the lake was deep, indicate substantial population sizes. The rapid input of inorganic materials during 4500–3000 cal BP flattened the depression in which DL had formed and resulted in a shallow peat bog that was colonized by macrophytes. The absence of *Isoetes* spores during 3000–2400 cal BP and 1500–1400 cal BP indicates the disappearance of the species from DL. It appears that *I. taiwanensis* populations are very vulnerable in shallow peat bog environments.

The annual mean water depth is strongly associated with the population dynamics of the species in DL [3]. We calculated the peat accumulation rate to evaluate the terrestrialization of the site. Today, the annual mean water depth of DL is 39.4 cm. If the deposition rate remains at the current 0.03 cm y^{-1}, the site will have filled in in ~1300 years' time. The lowest mean water depth for survival of *I. taiwanensis* is 30 cm, suggesting that this endangered species may only continue to survive in DL for ~300 years. This may in fact be an overestimate, because the expansion of macrophytes during dry periods can accelerate terrestrialization through bioaccumulation [54]. In addition, judging from our finding that *Isoetes* spores dominated below 100 cm, the ideal mean water depth for *I. taiwanensis* is probably deeper than 140 cm [3].

The coverage area of *I. taiwanensis* in DL is negatively correlated with the duration of dry-lake conditions (Figure 2). Extended dry-lake periods may reduce the ability of the species to compete with submerged and terrestrial plants [3]. Sufficient precipitation in the dry (winter) season can mitigate dry-lake conditions and increase *I. taiwanensis* populations. Fire frequency is negatively correlated with *Isoetes* spore density (Figure 8), suggesting that intense East Asian winter monsoon (EAWM) precipitation positively affects the species' population. According to model simulations, the weakening of the EAWM is likely to be more pronounced under global warming trends [55]. It is therefore likely that the threat of extinction facing *I. taiwanensis* in the wild will intensify in the future.

The arrival of *I. taiwanensis* in DL is thought to be due to spores or plants having been carried in by migratory waterfowl [6]. Our records reveal recolonization by the species after drought-induced disturbances, underscoring the importance of this dispersal process. However, this natural reintroduction mechanism has now been lost, since DL is the last remaining natural habitat of *I. taiwanensis*.

Isoetes species are characterized by geographically restricted ranges and feature a great many locally derived endemics that are subject to long-distance dispersal by waterfowl [56]. Based on molecular phylogenetic relationships, *I. taiwanensis* may be the ancestor of three other *Isoetes* species occurring in Japan and Korea, although their geographic distributions do not overlap [57]. The decline and extirpation of *Isoetes* species in East Asia, resulting from habitat degradation and loss, water pollution and eutrophication, competitive exclusion, and human disturbance, could be the main factors causing the biogeographical gaps between the ranges of these taxa [58]. A detailed palynological study of *Isoetes* species in East Asia may fill in these gaps and clarify the evolutionary history of this genus through the evidence provided by their subfossil spores. This may supply the spatiotemporal distribution of *Isoetes* species, which constitutes an important scientific basis for a reintroduction and recovery plan.

5. Conclusions

The multidecadal pollen record from DL suggests that changes in local vegetation and lacustrine conditions in northern Taiwan are linked to regional climate patterns, driven mainly by EASM intensity. The lack of volcanic ash and anthropogenic pollen indicators in the DL sediments suggests a low impact of volcanic and human activity on local vegetation during 4500–400 cal BP. Local floristic diversity seems sensitive to wildfire disturbances, which is negatively correlated with EAWM intensity. Our results suggest that reintroduction via waterfowl after a long-term dry period is a critical mechanism of reducing the risk of extinction for *Isoetes taiwanensis*. Based on our findings, the risk of floristic diversity degradation and *I. taiwanensis* extinction will increase significantly, because of decreased EAWM precipitation under future global warming scenarios. We recommend that conservation decision-makers at Yangmingshan National Park consider both paleoecological and more recent observational data when planning restoration strategies.

Funding: This research was funded by the Ministry of Science and Technology, Taiwan, grant number MOST 108-2116-M-194-003-, MOST 109-2116-M-194-011-, and MOST 110-2116-M-194-008-.

Institutional Review Board Statement: Not applicable.

Informed Consent Statement: Not applicable.

Data Availability Statement: The data presented in this study are available on request from the corresponding author.

Acknowledgments: We thank Meng-Yang Lee, Zih-Wei Tang, and Kang-Yu Fan for their help in core drilling and field excursion. We thank Yangmingshan National Park Headquarters for its permission to sample in DL and providing the GIS data of regional and local vegetation. We thank NTUAMS ^{14}C Dating Lab of Taiwan for the radiocarbon measurements.

Conflicts of Interest: The authors declare no conflict of interest.

References

1. Roleček, J.; Svitavská Svobodová, H.; Jamrichová, E.; Dudová, L.; Hájková, P.; Kletetschka, G.; Kuneš, P.; Abraham, V. Conservation Targets from the Perspective of a Palaeoecological Reconstruction: The Case Study of Dářko Peat Bog in the Czech Republic. *Preslia* **2020**, *92*, 87–114. [CrossRef]
2. Lin, C.-H.; Shih, M.-H.; Lai, Y.-C. Mantle Wedge Diapirs Detected by a Dense Seismic Array in Northern Taiwan. *Sci. Rep.* **2021**, *11*, 1561. [CrossRef]
3. Yu, Y.-T.; Lur, H.-S.; Chang, W.-L. Association of Water Depth and Aquatic-Plant Competition in Conservation of Isoetes Taiwanensis in the Menghuan Pond Wetland in Taiwan. *Paddy Water Environ.* **2013**, *11*, 513–519. [CrossRef]
4. Chen, S.-H.; Wu, J.-T.; Yang, T.-N.; Chuang, P.-P.; Huang, S.-Y.; Wang, Y.-S. Late Holocene Paleoenvironmental Changes in Subtropical Taiwan Inferred from Pollen and Diatoms in Lake Sediments. *J. Paleolimnol.* **2009**, *41*, 315–327. [CrossRef]
5. Huang, T.C.; Chen, H.J. The Pollen Analysis of the Dream Lake, Taipei, Yang Ming Shan National Park. *J. Palynol.* **1988**, *23*, 213–216.
6. Huang, T.-C.; Chen, H.-J.; Li, L.-C. A Palynological Study of *Isoëtes taiwanensis* DeVol. *Am. Fern J.* **1992**, *82*, 142–150. [CrossRef]
7. Wang, L.-C.; Chang, Y.-P.; Li, H.-C.; Chen, S.-H.; Wu, J.-T.; Lee, T.-Q.; Shiau, L.-J. Revealing the Vegetation, Fire and Human Activities in the Lowland of Eastern Taiwan during Late Holocene. *Quat. Int.* **2020**, *544*, 32–40. [CrossRef]
8. Belousov, A.; Belousova, M.; Chen, C.-H.; Zellmer, G.F. Deposits, Character and Timing of Recent Eruptions and Gravitational Collapses in Tatun Volcanic Group, Northern Taiwan: Hazard-Related Issues. *J. Volcanol. Geotherm. Res.* **2010**, *191*, 205–221. [CrossRef]
9. Chen, S.H.; Huang, S.Y. Aeropalynological Study of Yangminshan National Park, Taiwan. *Taiwania* **2000**, *45*, 281–295.
10. Lin, H.-J. *Investigation and Monitoring of Habitats in Mengxiang Lake Ecological Reserve in Yangmingshan National Park*; Yangmingshan National Park Headquarters: Taipei, Taiwan, 2015.
11. The R Development Core Team. *R: A Language and Environment for Statistical Computing*; R Foundation for Statistical Computing: Vienna, Austria, 2015.
12. Blaauw, M.; Christen, J.A. Flexible Paleoclimate Age-Depth Models Using an Autoregressive Gamma Process. *Bayesian Anal.* **2011**, *6*, 457–474. [CrossRef]
13. Reimer, P.J.; Austin, W.E.N.; Bard, E.; Bayliss, A.; Blackwell, P.G.; Ramsey, C.B.; Butzin, M.; Cheng, H.; Edwards, R.L.; Friedrich, M.; et al. The IntCal20 Northern Hemisphere Radiocarbon Age Calibration Curve (0–55 Cal KBP). *Radiocarbon* **2020**, *62*, 725–757. [CrossRef]
14. Huang, T.-C. *Pollen Flora of Taiwan*; National Taiwan University Botany Department Press: Taipei, Taiwan, 1972; p. 297.
15. Huang, T.-C. *Spore Flora of Taiwan*; National Taiwan University Botany Department Press: Taipei, Taiwan, 1981; p. 111.
16. Grimm, E.C. CONISS: A FORTRAN 77 Program for Stratigraphically Constrained Cluster Analysis by the Method of Incremental Sum of Squares. *Comput. Geosci.* **1987**, *13*, 13–35. [CrossRef]
17. Birks, H.J.B.; Felde, V.A.; Bjune, A.E.; Grytnes, J.-A.; Seppä, H.; Giesecke, T. Does Pollen-Assemblage Richness Reflect Floristic Richness? A Review of Recent Developments and Future Challenges. *Rev. Palaeobot. Palynol.* **2016**, *228*, 1–25. [CrossRef]
18. Liang, C.; Zhao, Y.; Qin, F.; Cui, Q.-Y.; Li, Q.; Li, H.; Zhang, Z.-Y. Complex Responses of Vegetation Diversity to Holocene Climate Change in the Eastern Tibetan Plateau. *Veg. Hist. Archaeobotany* **2019**, *28*, 379–390. [CrossRef]
19. Matthias, I.; Semmler, M.S.S.; Giesecke, T. Pollen Diversity Captures Landscape Structure and Diversity. *J. Ecol.* **2015**, *103*, 880–890. [CrossRef]
20. Gosling, W.D.; Julier, A.C.M.; Adu-Bredu, S.; Djagbletey, G.D.; Fraser, W.T.; Jardine, P.E.; Lomax, B.H.; Malhi, Y.; Manu, E.A.; Mayle, F.E.; et al. Pollen-Vegetation Richness and Diversity Relationships in the Tropics. *Veg. Hist. Archaeobotany* **2018**, *27*, 411–418. [CrossRef]
21. Schwörer, C.; Colombaroli, D.; Kaltenrieder, P.; Rey, F.; Tinner, W. Early Human Impact (5000–3000 BC) Affects Mountain Forest Dynamics in the Alps. *J. Ecol.* **2015**, *103*, 281–295. [CrossRef]
22. Jantz, N.; Behling, H. A Holocene Environmental Record Reflecting Vegetation, Climate, and Fire Variability at the Páramo of Quimsacocha, Southwestern Ecuadorian Andes. *Veg. Hist. Archaeobotany* **2012**, *21*, 169–185. [CrossRef]
23. McGlinn, D.J.; Xiao, X.; May, F.; Gotelli, N.J.; Engel, T.; Blowes, S.A.; Knight, T.M.; Purschke, O.; Chase, J.M.; McGill, B.J. Measurement of Biodiversity (MoB): A Method to Separate the Scale-Dependent Effects of Species Abundance Distribution, Density, and Aggregation on Diversity Change. *Methods Ecol. Evol.* **2019**, *10*, 258–269. [CrossRef]
24. Whitlock, C.; Larsen, C. Charcoal as a Fire Proxy. In *Tracking Environmental Change Using Lake Sediments*; Smol, J.P., Birks, H.J.B., Last, W.M., Bradley, R.S., Alverson, K., Eds.; Kluwer Academic Publishers: Dordrecht, The Netherlands, 2002; Volume 3, pp. 75–97. ISBN 1-4020-0681-0.
25. Rueden, C.T.; Schindelin, J.; Hiner, M.C.; DeZonia, B.E.; Walter, A.E.; Arena, E.T.; Eliceiri, K.W. ImageJ2: ImageJ for the next Generation of Scientific Image Data. *BMC Bioinform.* **2017**, *18*, 529. [CrossRef]
26. Higuera, P.E.; Brubaker, L.B.; Anderson, P.M.; Hu, F.S.; Brown, T.A. Vegetation Mediated the Impacts of Postglacial Climate Change on Fire Regimes in the South-Central Brooks Range, Alaska. *Ecol. Monogr.* **2009**, *79*, 201–219. [CrossRef]
27. Hsu, L.-T. *The Study of the Vegetation Changes in Yangmingshan National Park*; Yangmingshan National Park Headquarters: Taipei, Taiwan, 2008; p. 121.
28. Woodward, C.; Haines, H.A. Unprecedented Long-Distance Transport of Macroscopic Charcoal from a Large, Intense Forest Fire in Eastern Australia: Implications for Fire History Reconstruction. *Holocene* **2020**, *30*, 947–952. [CrossRef]

29. Conedera, M.; Tinner, W.; Neff, C.; Meurer, M.; Dickens, A.F.; Krebs, P. Reconstructing Past Fire Regimes: Methods, Applications, and Relevance to Fire Management and Conservation. *Quat. Sci. Rev.* **2009**, *28*, 555–576. [CrossRef]
30. Bunting, M.J.; Gaillard, M.-J.; Sugita, S.; Middleton, R.; Broström, A. Vegetation Structure and Pollen Source Area. *The Holocene* **2004**, *14*, 651–660. [CrossRef]
31. Conedera, M.; Tinner, W.; Crameri, S.; Torriani, D.; Herold, A. Taxon-Related Pollen Source Areas for Lake Basins in the Southern Alps: An Empirical Approach. *Veg. Hist. Archaeobotany* **2006**, *15*, 263–272. [CrossRef]
32. Liew, P.-M.; Wu, M.-H.; Lee, C.-Y.; Chang, C.-L.; Lee, T.-Q. Recent 4000 Years of Climatic Trends Based on Pollen Records from Lakes and a Bog in Taiwan. *Quat. Int.* **2014**, *349*, 105–112. [CrossRef]
33. Luo, C.; Chen, M.; Xiang, R.; Liu, J.; Zhang, L.; Lu, J.; Yang, M. Modern Pollen Distribution in Marine Sediments from the Northern Part of the South China Sea. *Mar. Micropaleontol.* **2014**, *108*, 41–56. [CrossRef]
34. Lee, C.-Y.; Liew, P.-M.; Lee, T.-Q. Pollen Records from Southern Taiwan: Implications for East Asian Summer Monsoon Variation during the Holocene. *Holocene* **2010**, *20*, 81–89. [CrossRef]
35. Wang, L.-C.; Wu, J.-T.; Lee, T.-Q.; Lee, P.-F.; Chen, S.-H. Climate Changes Inferred from Integrated Multi-Site Pollen Data in Northern Taiwan. *J. Asian Earth Sci.* **2011**, *40*, 1164–1170. [CrossRef]
36. Wang, L.-C.; Behling, H.; Kao, S.-J.; Li, H.-C.; Selvaraj, K.; Hsieh, M.-L.; Chang, Y.-P. Late Holocene Environment of Subalpine Northeastern Taiwan from Pollen and Diatom Analysis of Lake Sediments. *J. Asian Earth Sci.* **2015**, *114*, 447–456. [CrossRef]
37. Wang, L.-C.; Tang, Z.-W.; Chen, H.-F.; Li, H.-C.; Shiau, L.-J.; Huang, J.-J.S.; Wei, K.-Y.; Chuang, C.-K.; Chou, Y.-M. Late Holocene Vegetation, Climate, and Natural Disturbance Records from an Alpine Pond in Central Taiwan. *Quat. Int.* **2019**, *528*, 63–72. [CrossRef]
38. Huang, Z.; Ma, C.; Chyi, S.-J.; Tang, L.; Zhao, L. Paleofire, Vegetation, and Climate Reconstructions of the Middle to Late Holocene From Lacustrine Sediments of the Toushe Basin, Taiwan. *Geophys. Res. Lett.* **2020**, *47*, e2020GL090401. [CrossRef]
39. Zhao, K.; Wang, Y.; Edwards, R.L.; Cheng, H.; Liu, D.; Kong, X. A High-Resolved Record of the Asian Summer Monsoon from Dongge Cave, China for the Past 1200 Years. *Quat. Sci. Rev.* **2015**, *122*, 250–257. [CrossRef]
40. Zhang, Z.; Yao, Q.; Liu, K.; Li, L.; Yin, R.; Wang, G.; Sun, J. Historical Flooding Regime along the Amur River and Its Links to East Asia Summer Monsoon Circulation. *Geomorphology* **2021**, *388*, 107782. [CrossRef]
41. Manville, V.; Hodgson, K.A.; Nairn, I.A. A Review of Break-out Floods from Volcanogenic Lakes in New Zealand. *N. Z. J. Geol. Geophys.* **2007**, *50*, 131–150. [CrossRef]
42. Wang, L.-C.; Behling, H.; Chen, Y.-M.; Huang, M.-S.; Chen, C.-T.A.; Lou, J.-Y.; Chang, Y.-P.; Li, H.-C. Holocene Monsoonal Climate Changes Tracked by Multiproxy Approach from a Lacustrine Sediment Core of the Subalpine Retreat Lake in Taiwan. *Quat. Int.* **2014**, *333*, 69–76. [CrossRef]
43. Wang, L.-C.; Behling, H.; Lee, T.-Q.; Li, H.-C.; Huh, C.-A.; Shiau, L.-J.; Chang, Y.-P. Late Holocene Environmental Reconstructions and Their Implications on Flood Events, Typhoon, and Agricultural Activities in NE Taiwan. *Clim. Past* **2014**, *10*, 1857–1869. [CrossRef]
44. Tang, L.; Mao, L.; Lü, X.; Ma, Q.; Zhou, Z.; Yang, C.; Kong, Z.; Batten, D.J. Palaeoecological and Palaeoenvironmental Significance of Some Important Spores and Micro-Algae in Quaternary Deposits. *Chin. Sci. Bull.* **2013**, *58*, 3125–3139. [CrossRef]
45. Wang, L.-C.; Chou, Y.-M.; Chen, H.-F.; Chang, Y.-P.; Chiang, H.-W.; Yang, T.-N.; Shiau, L.-J.; Chen, Y.-G. Paleolimnological Evidence for Lacustrine Environmental Evolution and Paleo-Typhoon Records during the Late Holocene in Eastern Taiwan. *J. Paleolimnol.* **2021**. [CrossRef]
46. Park, J.; Han, J.; Jin, Q.; Bahk, J.; Yi, S. The Link between ENSO-like Forcing and Hydroclimate Variability of Coastal East Asia during the Last Millennium. *Sci. Rep.* **2017**, *7*, 8166. [CrossRef]
47. Thompson, D.M.; Conroy, J.L.; Collins, A.; Hlohowskyj, S.R.; Overpeck, J.T.; Riedinger-Whitmore, M.; Cole, J.E.; Bush, M.B.; Whitney, H.; Corley, T.L.; et al. Tropical Pacific Climate Variability over the Last 6000 Years as Recorded in Bainbridge Crater Lake, Galápagos. *Paleoceanography* **2017**, *32*, 903–922. [CrossRef]
48. Cheng, H.; Edwards, R.L.; Sinha, A.; Spötl, C.; Yi, L.; Chen, S.; Kelly, M.; Kathayat, G.; Wang, X.; Li, X.; et al. The Asian Monsoon over the Past 640,000 Years and Ice Age Terminations. *Nature* **2016**, *534*, 640–646. [CrossRef] [PubMed]
49. Yeh, Y.-L.; Wang, W.-H.; Wen, S. Dense Seismic Arrays Deny a Massive Magma Chamber beneath the Taipei Metropolis, Taiwan. *Sci. Rep.* **2021**, *11*, 1083. [CrossRef] [PubMed]
50. de Porras, M.E.; Maldonado, A.; Abarzúa, A.M.; Cárdenas, M.L.; Francois, J.P.; Martel-Cea, A.; Stern, C.R.; Méndez, C.; Reyes, O. Postglacial Vegetation, Fire and Climate Dynamics at Central Chilean Patagonia (Lake Shaman, 44° S). *Quat. Sci. Rev.* **2012**, *50*, 71–85. [CrossRef]
51. Lee, C.-Y.; Chang, C.-L.; Liew, P.-M.; Lee, T.-Q.; Song, S.-R. Climate Change, Vegetation History, and Agricultural Activity of Lake Li-Yu Tan, Central Taiwan, during the Last 2.6 Ka BP. *Quat. Int.* **2014**, *325*, 105–110. [CrossRef]
52. Wenske, D.; Böse, M.; Frechen, M.; Lüthgens, C. Late Holocene Mobilisation of Loess-like Sediments in Hohuan Shan, High Mountains of Taiwan. *Quat. Int.* **2011**, *234*, 174–181. [CrossRef]
53. Fang, K.; Yao, Q.; Guo, Z.; Zheng, B.; Du, J.; Qi, F.; Yan, P.; Li, J.; Ou, T.; Liu, J.; et al. ENSO Modulates Wildfire Activity in China. *Nat. Commun.* **2021**, *12*, 1764. [CrossRef] [PubMed]
54. Zhang, Y.; Cui, B.; Lan, Y.; Han, Z.; Wang, T.; Guo, A. Four Terrestrialization Characteristics of Baiyangdian Lake, China. *Procedia Environ. Sci.* **2012**, *13*, 645–654. [CrossRef]

55. Gong, H.; Wang, L.; Zhou, W.; Chen, W.; Wu, R.; Liu, L.; Nath, D.; Leung, M.Y.-T. Revisiting the Northern Mode of East Asian Winter Monsoon Variation and Its Response to Global Warming. *J. Clim.* **2018**, *31*, 9001–9014. [CrossRef]
56. Taylor, W.C.; Hickey, R.J. Habitat, Evolution, and Speciation in Isoetes. *Ann. MO Bot. Gard.* **1992**, *79*, 613–622. [CrossRef]
57. Kim, C.; Shin, H.; Chang, Y.-T.; Choi, H.-K. Speciation Pathway of *Isoëtes* (Isoëtaceae) in East Asia Inferred from Molecular Phylogenetic Relationships. *Am. J. Bot.* **2010**, *97*, 958–969. [CrossRef] [PubMed]
58. Liu, X.; Wang, J.-Y.; Wang, Q.-F. Current Status and Conservation Strategies for *Isoetes* in China: A Case Study for the Conservation of Threatened Aquatic Plants. *Oryx* **2005**, *39*, 335–338. [CrossRef]